Acta Mechanica 87, 123—133 (1991)

ACTA MECHANICA

New integral equation in the thin airfoil problem

S. W. Zhang and Y. Z. Chen, Jiangsu, People's Republic of China

(Received June 5, 1990; revised September 24, 1990)

Summary. A new integral equation concerning the thin airfoil problem is proposed. In this equation, the unknown function represents vorticity along the thin airfoil, and the right hand term of the equation is chosen as the stream function in two-dimensional potential flow. The equation has a logarithm kernel with a weaker singularity than the known one [1]. After solution of the integral equation, i.e. after determination of vorticity, the lift forces and moment acting on the thin airfoil can be calculated immediately, as it follows from the Blasius's formulae. Several numerical examples are given.

1 Introduction

The theory of potential two-dimensional flow (abbreviated as PTDF) has history of more than a hundred of years. In this theory, the so called "thin airfoil problem" occuring in theoretical aerodynamics, used to play an important role. Several approaches for solving this problem as well as other problems in PTDF were suggested [1]—[7]. In an earlier approach to the thin airfoil problem, after replacing the airfoil with its camber line, and assuming the density of vorticity along the chord line as unknown function, and introducing the normal velocity with respect to the thin airfoil in the impermeability condition, the well-known singular integral equation could be obtained [1], [2]. For the sake of simplicity, the following additional assumptions were usually imposed:

(1) the impermeability condition had to be satisfied on the x-axis (chord line) instead of the camber line,
(2) the angle of attack was small,
(3) the camber line $z = z(x)$ should satisfy the condition: $\arctan\left(\frac{dz}{dx}\right) \cong \frac{dz}{dx}$.

The integral equation was solved successfully [1], the singularity being taken care of by means of a suitable approximation of the vorticity function.

More recently, it was pointed out that the proper choice of a field quantity in solving boundary value problems in mechanics is of great importance [8], [9]. Assume that t is a source point in a plane and that t_0 is an "observation" point in the same plane. If the "observation" field quantity is chosen such that the influence is directly proportional to $(t - t_0)^{-1}$, then the following type of integral $\int \mu(s)\,(t - t_0)^{-1}$ (an integral along a curve) is involved in the resulting integral equation. Generally speaking, the above mentioned integral should be understood in the sense of the Cauchy integral. This is a usual difficulty encountered in the process of solving the boundary integral equation as well as the singular integral equation of the thin airfoil problem in PTDF.

Clearly, the character of the kernel in an integral equation depends on the choice both of the unknown function, and the right hand term of the integral equation. In this paper,

we still use the vortex density as the unknown function of the integral equation. Nevertheless, instead of the velocity component normal with respect to the camber line we use the stream function in the right hand term of the integral equation. In such a manner, an integral equation with the logarithm kernel, i.e. with "weaker" singularity can be obtained. As it is mentioned below, and as also cited in some references [8], [9], the numerical solution of the proposed integral equation is more easy and convenient to carry out.

2 Analysis

It is well known that, every two-dimensional incompressible potential flow is governed by a corresponding complex potential $W(z)$ [2], [3]

$$W(z) = \varphi(x, y) + i\psi(x, y), \tag{1}$$

where $\varphi(x, y)$ denotes the velocity potential and $\psi(x, y)$ the stream function. The both two functions $\varphi(x, y)$ and $\psi(x, y)$ are harmonic. The complex velocity of the flow is represented by the formulae [2], [3]

$$W'(z) = u - iv, \tag{2}$$

where u, v denote the velocity components in the x-, or y-direction, respectively. Of course:

$$u = \frac{\partial \varphi}{\partial x} = \frac{\partial \psi}{\partial y}; \qquad v = \frac{\partial \varphi}{\partial y} = -\frac{\partial \psi}{\partial x}. \tag{3}$$

In order to formulate the mentioned integral equation, the complex potential corresponding to a vortex filament placed at the point $z = t$ in Fig. 1 is introduced as

$$W(z) = \varphi(x, y) + i\psi(x, y) = iH \ln (z - t), \tag{4}$$

where H is real, and it represents the strength of the vortex filament at the point $z = t$ (Fig. 1). Let $\{g\}_t$ denote the contour increment of some function g for the closed path around the point $z = t$ in Fig. 1. From (1) and (4), we have

$$\{W\}_t = -2\pi H, \quad \text{or} \quad \{\varphi\}_t = -2\pi H, \quad \{\psi\}_t = 0. \tag{5}$$

Now let us consider the thin airfoil problem shown in Fig. 2. The air-foil is placed in an infinite continuum with the velocity components at infinity denoted by u_∞ and v_∞. Obviously, the investigated complex potential $W^*(z)$ can be decomposed as follows:

$$\begin{aligned} &W^*(z) = \varphi^*(x, y) + i\psi^*(x, y) = W_1(z) + W(z); \\ &W_1(z) = \varphi_1(x, y) + i\psi_1(x, y); \\ &W(z) = \varphi(x, y) + i\psi(x, y), \end{aligned} \tag{6}$$

where

$$W_1(z) = (u_\infty - iv_\infty)\, z = (xu_\infty + yv_\infty) + i(-xv_\infty + yu_\infty) \tag{7}$$

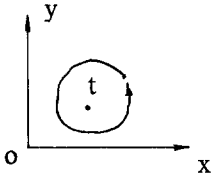

Fig. 1. A vortex filament placed at the point $z = t$

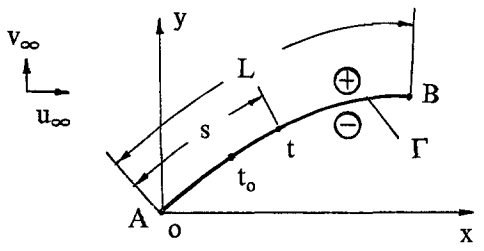

Fig. 2. A curved thin airfoil in the infinite continuum

represents the complex potential defined in the whole plane when the field has not been perturbed by the thin airfoil, and $W(z)$ represents the perturbation part of the complex potential.

It is easy to see that the normal velocity component should vanish along the thin airfoil (Γ in Fig. 2). It leads to the following boundary condition:

$$\frac{\partial \varphi^*}{\partial n} = \frac{\partial \varphi_1}{\partial n} + \frac{\partial \varphi}{\partial n} = 0, \qquad \text{(along } \Gamma \text{ in Fig. 2)}. \tag{8}$$

By means of using the Cauchy-Riemann condition, the equation (8) yields:

$$\frac{\partial \psi}{\partial s} = -\frac{\partial \psi_1}{\partial s}, \qquad \text{(along } \Gamma \text{ in Fig. 2)} \tag{9}$$

and after integration one obtains the following boundary condition for the perturbation field

$$\psi = -\psi_1 + c = xv_\infty - yu_\infty + c, \qquad \text{(along } \Gamma \text{ in Fig. 2)} \tag{10}$$

where c is an arbitrary constant.

The perturbation field can be described by vorticity $\mu(s)$ along the thin airfoil. Thus, if H in (4) is replaced by $\mu(s)\,ds$ and integration along Γ is carried out, we obtain the following complex potential

$$W(z) = i \int_0^L \mu(s) \ln (z - t)\, ds. \tag{11}$$

Let z approach the upper or lower border of the thin airfoil, i.e. $z \to t_0^+$ or $z \to t_0^-$. In either case, from equation (11) we have

$$\psi(s_0) = \int_0^L \mu(s) \ln \big(r(t, t_0)\big)\, ds, \qquad (s_0 \in \Gamma) \tag{12}$$

where $r(t, t_0)$ represents the distance between two point $z = t$ and $z = t_0$. Finally, from (10) and (12), a weaker singular integral equation with logarithm kernel is obtained as follows

$$\int_0^L \mu(s) \ln \big(r(t, t_0)\big)\, ds = x_0 v_\infty - y_0 u_\infty + c \qquad (t_0 = x_0 + iy_0). \tag{13}$$

The numerical solution of the above integral equation will be presented below. The lift Y, the drag X, and the moment M can be expressed by the known formulae: [2], [3]

$$\begin{aligned} Y + iX &= -\frac{\varrho}{2} \int_C \left(\frac{dW^*}{dz}\right)^2 dz; \\ M &= -\frac{\varrho}{2} \operatorname{Re} \int_C \left(\frac{dW^*}{dz}\right)^2 z\, dz, \end{aligned} \tag{14}$$

where C is any closed integration path around the thin airfoil, and ϱ denotes the fluid density.

Clearly, from (6), (7) and (11), the complex velocity of the whole field can be expressed by

$$\frac{dW^*}{dz} = u_\infty - iv_\infty + i\int_0^L \frac{\mu(s)\,ds}{z-t}. \tag{15}$$

Furthermore, the complex velocity at the infinity can be expressed as

$$\frac{dW^*}{dz} = u_\infty - iv_\infty + \frac{iA}{z} + \frac{iB}{z^2} + \cdots, \tag{16}$$

where

$$A = \int_0^L \mu(s)\,ds, \qquad B = B_1 + iB_2 = \int_0^L t\mu(s)\,ds. \tag{17}$$

After substituting (16) into (14) and using the residual theorem, one obtains

$$\begin{aligned} &Y + iX = 2\pi\varrho A(u_\infty - iv_\infty), \\ &M = 2\pi\varrho\ \mathrm{Re}\left(B(u_\infty - iv_\infty)\right) = 2\pi\varrho(B_1u_\infty + B_2v_\infty). \end{aligned} \tag{18}$$

Therefore, the thin airfoil problem in PTDF is reduced to solve the integral equation (13) and to evaluate the integrals (17). We introduce the formulae (14)—(18), because they will be used in the examples.

3 Numerical analysis and examples

As mentioned above, the main task in the present investigation is to solve the integral equation (13) numerically. In addition, the most important point in the numerical solution is to consider the following two particular features which appeared in the thin airfoil problem.

(a) The vortex density $\mu(s)$ has a $s^{-1/2}$ type singularity at the leading edge point A of the thin airfoil in Fig. 2. Meantime, from the Joukowski hypothesis, $\mu(s)$ becomes zero at the trailing edge point B in Fig. 2.

(b) In (13), if $t \to t_0$, the kernel $\ln\left(r(t, t_0)\right)$ has a logarithm type singularity. It is well known that the integrals containing the abovementioned singularity are integrable.

The integral (12) will be rewritten again for the sake of convenience:

$$I = \int_0^L \mu(s) \ln\left(r(t, t_0)\right) ds. \tag{19}$$

In the numerical approach to its evaluation, the thin airfoil will be approximated by a polygon consisting of N line segments P_1P_2, P_2P_3, ..., P_NP_{N+1} in Fig. 3.

In result of the above-mentioned approximation, the integral in (19) can be rewritten as

$$I = \sum_{j=1}^{N} I_j = \sum_{j=1}^{N} \int_{P_j}^{P_{j+1}} \ln\left(r(t, t_0)\right) \mu(s)\,ds. \tag{20}$$

The interpolation formulae for $\mu(s)$ are of three kinds. For the first segment (P_1P_2 in Fig. 3), the following interpolation formula in the local coordinate s_1 has been found to be

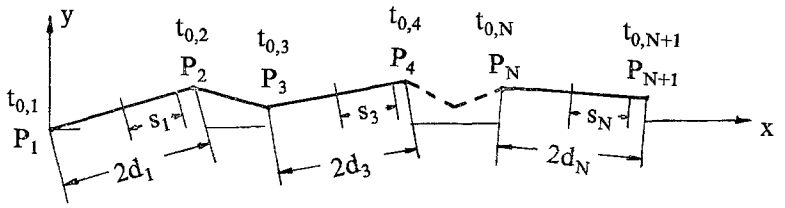

Fig. 3. A polygon approximating the thin airfoil

suitable [8]

$$\mu(s_1) = \mu_1\left(\sqrt{\frac{2d_1}{d_1 + s_1}} - 1\right) + \mu_2 \qquad (|s_1| < d_1). \tag{21}$$

The above interpolation formula reflects the nature of $\mu(s)$ at the leading edge of the thin airfoil and satisfies the following condition

$$\mu(s_1)|_{s_1 = d_1} = \mu_2. \tag{22}$$

In the intermediate segments (from P_2P_3 to $P_{N-1}P_N$ in Fig. 3), the following interpolation formula for $\mu(s)$, for example along P_3P_4, is assumed

$$\mu(s_3) = \frac{1}{2}\left(\mu_3(1 - s_3/d_3) + \mu_4(1 + s_3/d_3)\right) \qquad (|s_3| < d_3). \tag{23}$$

Finally, at the last segment (P_NP_{N+1} in Fig. 3), the following interpolation formula is suggested

$$\mu(s_N) = \frac{1}{2}\mu_N(1 - s_N/d_N) \qquad (|s_N| < d_N). \tag{24}$$

The above representation reflects the nature of $\mu(s)$ at the trailing edge (P_{N+1} in Fig. 3).

If the above interpolation formulae for $\mu(s)$ are used, the integration indicated in (20) can be separated into the following types

$$J_1 = \int_0^{2d} \left((2d/r)^{1/2} - 1\right) \ln r \, dr = 2d\left(\ln(2d) - 3\right),$$

$$J_2 = \int_0^{2d} \ln r \, dr = 2d\left(\ln(2d) - 1\right),$$

$$J_3 = \int_0^{2d} \left((2d/r)^{1/2} - 1\right) \ln(2d - r) \, dr = 2d\left(\ln(2d) - 3 + 4\ln(2d)\right),$$

$$J_4 = \int_0^{2d} (1 - r/2d) \ln r \, dr = d\left(\ln(2d) - 1.5\right), \tag{25.1—7}$$

$$J_5 = \int_0^{2d} (r/2d) \ln r \, dr = d\left(\ln(2d) - 0.5\right),$$

$$J_6 = \int_{-d}^{d} g(s)/(d^2 - s^2)^{1/2} \, ds,$$

$$J_7 = \int_{-d}^{d} h(s) \, ds.$$

The first five integrals have been integrated in a closed form. In addition, the integrals (25.1) and (25.2) can be integrated by the use of the following Chebyshev integration rule

$$\int_{-d}^{d} g(s)/(d^2 - s^2)^{1/2}\, ds = \frac{\pi}{M} \sum_{m=1}^{M} g(s_m), \qquad s_m = d \cos\left(\frac{2m-1}{2M}\pi\right), \qquad m = 1, 2, \ldots M. \tag{26}$$

Assuming that the integral equation (13) has to be satisfied at $N+1$ discrete points P_i (or $t_{0,i}$) $i = 1, 2, \ldots, N+1$, the following system of algebraic equations for $N+1$ unknowns $\mu_{0,1}, \mu_{0,2}, \ldots, \mu_{0,N}$ and c can be derived:

$$\sum_{j=1}^{N} \int_{P_j}^{P_{j+1}} \ln\left(r(t, t_{0,i})\right) \mu(s)\, ds - c = x_{0,i} v_\infty - y_{0,i} u_\infty, \qquad i = 1, 2, \ldots, N+1. \tag{27}$$

With no loss of generality, the leading edge (point P_1 in Fig. 3) can be assumed as coinciding with the origin of the coordinate system. Thus, $t_{0,1} = x_{0,1} + iy_{0,1} = 0$. By subtracting the first equation in (27) ($i = 1$) from the remaining ones ($i = 2, 3, \ldots, N+1$), an alternative form of the system of algebraic equations for the N unknowns $\mu_{0,1}, \mu_{0,2}, \ldots, \mu_{0,N}$ is obtained:

$$\sum_{j=1}^{N} \int_{P_j}^{P_{j+1}} \left\{\ln\left(r(t, t_{0,i})\right) - \ln\left(r(t, 0)\right)\right\} \mu(s)\, ds = x_{0,i} v_\infty - y_{0,i} u_\infty, \qquad i = 2, 3, \ldots, N+1. \tag{28}$$

The same interpolation formulae can be applied to evaluation of the integrals in (17). Four numerical examples will be presented in order to demonstrate the flexibility and accuracy of the proposed approach.

3.1 An inclined plate in flow uniform at infinity (Fig. 4)

A plate of the length $2a$ is placed in the flow uniform at infinity, and possessing the velocity u_∞ ($v_\infty = 0$). With respect to the assumed coordinate system, the plate is inclined at the angle α. The problem can be solved in closed form, i.e. the formulae (18) reduce in this case to the following solution:

$$\begin{aligned} X &= 0, \\ Y &= 2\pi\varrho a u_\infty^2 \sin\alpha, \\ M_c &= -\pi\varrho a^2 u_\infty^2 \sin\alpha \cos\alpha. \end{aligned} \tag{29}$$

We take $N = 10$ and $N = 20$ in (20), $M = 13$ in (26). The results are expressed as

$$\begin{aligned} Y &= f_1(\alpha)\, 2\pi\varrho a u_\infty^2, \qquad X = 0, \\ M_c &= -f_2(\alpha)\, \pi\varrho a^2 u_\infty^2. \end{aligned} \tag{30}$$

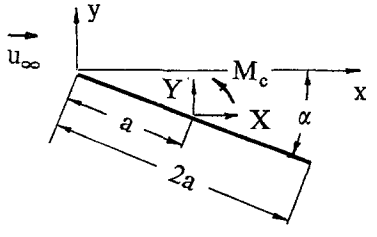

Fig. 4. An inclined plate in potential flow

Table 1. Calculated $f_1(\alpha)$ and $f_2(\alpha)$ values (see (29) and (30)).

α	0°	5°	10°	15°	20°	25°	30°	35°	40°
f_1 ($N = 10$)	0.000	0.086	0.172	0.256	0.338	0.417	0.494	0.567	0.635
f_1 ($N = 20$)	0.000	0.087	0.172	0.257	0.340	0.420	0.497	0.570	0.638
f_1 (exact)	0.000	0.087	0.174	0.259	0.342	0.423	0.500	0.574	0.643
f_2 ($N = 10$)	0.000	0.087	0.171	0.250	0.321	0.383	0.433	0.470	0.492
f_2 ($N = 20$)	0.000	0.087	0.171	0.250	0.321	0.383	0.433	0.470	0.492
f_2 (exact)	0.000	0.087	0.171	0.250	0.321	0.383	0.433	0.470	0.492

α	45°	50°	55°	60°	65°	70°	75°	80°	85°
f_1 ($N = 10$)	0.698	0.757	0.809	0.855	0.895	0.928	0.954	0.973	0.984
f_1 ($N = 20$)	0.702	0.761	0.813	0.860	0.900	0.933	0.959	0.978	0.990
f_1 (exact)	0.707	0.766	0.819	0.866	0.906	0.940	0.966	0.985	0.996
f_2 ($N = 10$)	0.500	0.492	0.470	0.433	0.383	0.321	0.250	0.171	0.087
f_2 ($N = 20$)	0.500	0.492	0.469	0.433	0.383	0.321	0.250	0.171	0.087
f_2 (exact)	0.500	0.492	0.470	0.433	0.383	0.321	0.250	0.171	0.087

The calculated values $f_1(\alpha)$ and $f_2(\alpha)$ and the ones obtained from the exact solution are listed in Table 1. As we see, the difference between numerical solution and exact solution is very small.

3.2 A parabolic arc in flow uniform at infinity (Fig. 5)

In the second example, the thin airfoil is approximated by a segment of a parabola. In the $x_1 \circ y_1$ coordinate system, the parabola can be expressed as

$$y_1 = \varepsilon(2ax_1 - x_1^2)/a. \tag{31}$$

The thin airfoil has an inclination angle α with respect to the x-axis (Fig. 5). It is assumed that, the velocity at infinity is u_∞ ($v_\infty = 0$). As before, we take $N = 20$ in (20) and $M = 13$ in (26). The calculated results are expressed by:

$$\begin{aligned} Y &= 2\pi\varrho a u_\infty^2 g_1(\alpha, \varepsilon), \qquad X = 0, \\ M_c &= -\pi\varrho a^2 u_\infty^2 g_2(\alpha, \varepsilon). \end{aligned} \tag{32}$$

In the above equation, the lift Y and moment M_c are applied at the point with the coordinates ($a \cos\alpha$, $-a \sin\alpha$). The calculated $g_1(\alpha, \varepsilon)$ and $g_2(\alpha, \varepsilon)$ values are plotted in Fig. 6 and Fig. 7, respectively.

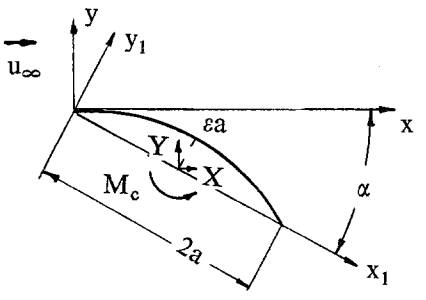

Fig. 5. A thin airfoil with parabola configuration in the potential flow

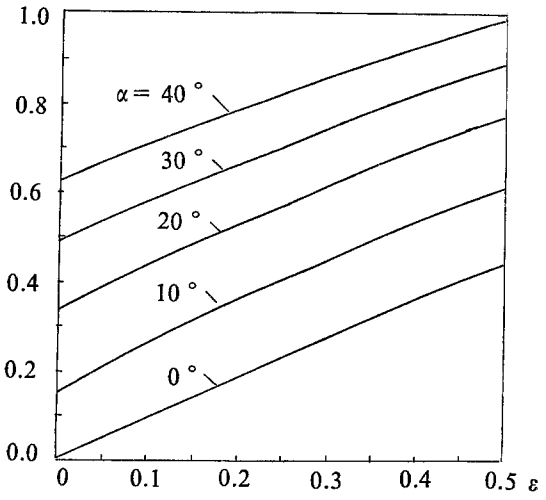

Fig. 6. $g_1(\alpha, \varepsilon)$ values in Eq. (32) (see Fig. 5)

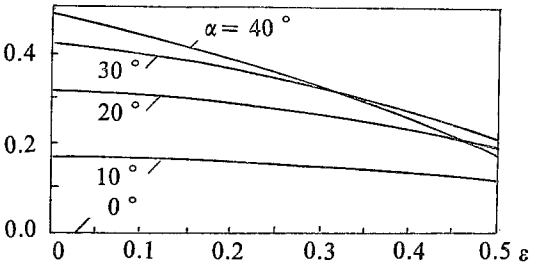

Fig. 7. $g_2(\alpha, \varepsilon)$ values in Eq. (32) (see Fig. 5)

3.3 A thin airfoil with a flap in the flow uniform at infinity (Fig. 8)

In the third example, a thin airfoil with kinked configuration is placed in the uniform flow with the velocity u_∞ ($v_\infty = 0$). The results are expressed by

$$\begin{aligned} Y &= 2\pi\varrho a u_\infty^2 h_1(\alpha, \beta), \qquad X = 0, \\ M_c &= -\pi\varrho a^2 u_\infty^2 h_2(\alpha, \beta). \end{aligned} \tag{33}$$

The calculated $h_1(\alpha, \beta)$ and $h_2(\alpha, \beta)$ values are plotted in Fig. 9 and Fig. 10, respectively.

Clearly, the relation between α and β for zero lift force ($Y = 0$) can be found from (33) and takes the form

$$h_1(\alpha, \beta) = 0. \tag{34}$$

From Fig. 8 we see that

$$h_1(\alpha, \beta)|_{\alpha=0°, \beta=0°} = 0, \quad \text{and} \quad h_1(\alpha, \beta)|_{\alpha=10°, \beta=-26°} = 0. \tag{35}$$

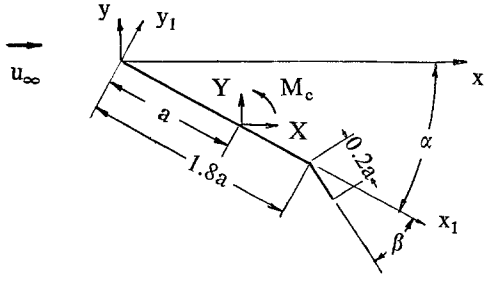

Fig. 8. A thin airfoil with kinked configuration in the potential flow

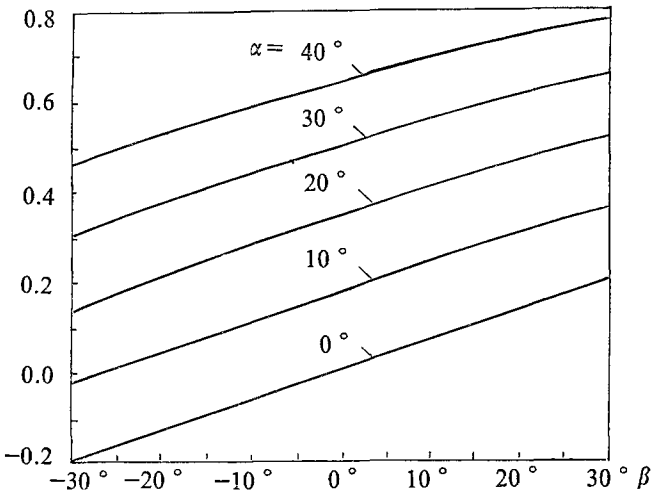

Fig. 9. $h_1(\alpha, \beta)$ values in Eq. (33) (see Fig. 8)

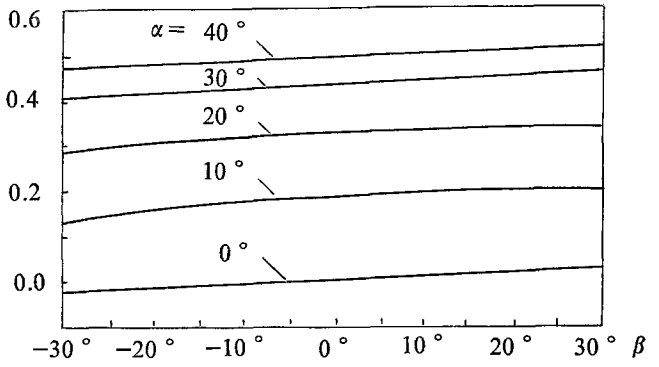

Fig. 10. $h_2(\alpha, \beta)$ values in Eq. (33) (see Fig. 8)

This is to say, in the vicinity of $\alpha = 0°$, $\beta = 0°$, we have the following zero lift force condition

$$\frac{\Delta\alpha}{\Delta\beta} = -10.0/26.0 = -0.385. \tag{36}$$

In the same condition, the ratio $\Delta\alpha/\Delta\beta$ reported previously takes the value −0.39 [2, p. 136 Fig. 18, when $E = 0.1$].

3.4 A thin airfoil with sine configuration in the uniform flow (Fig. 11)

In the fourth example, the sine configuration is expressed by

$$y_1 = \varepsilon a \sin(\pi x_1/a). \tag{37}$$

The calculated results are expressed by

$$\begin{aligned} Y &= 2\pi\varrho a u_\infty^2 k_1(\alpha, \varepsilon), \qquad X = 0, \\ M_c &= -\pi\varrho a^2 u_\infty^2 k_2(\alpha, \varepsilon). \end{aligned} \tag{38}$$

The calculated $k_1(\alpha, \varepsilon)$ and $k_2(\alpha, \varepsilon)$ values are plotted in Fig. 12 and Fig. 13 respectively.

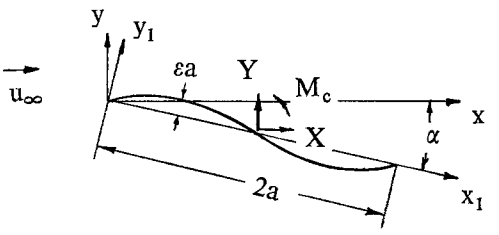

Fig. 11. A thin airfoil with sine configuration in the potential flow

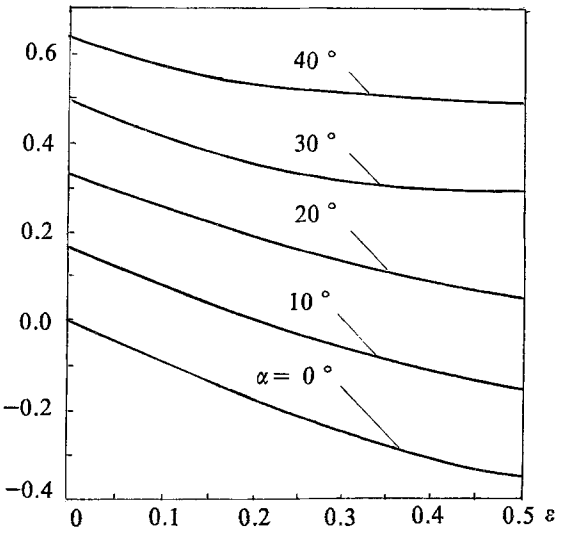

Fig. 12. $k_1(\alpha, \varepsilon)$ values in Eq. (38) (see Fig. 11)

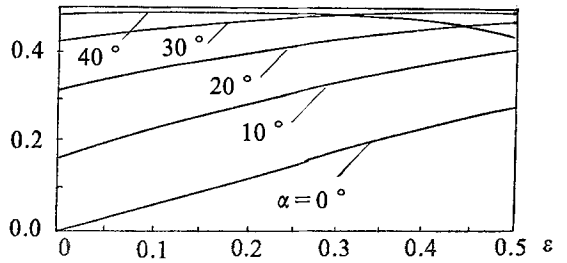

Fig. 13. $k_2(\alpha, \varepsilon)$ values in Eq. (38) (see Fig. 11)

As before, from Fig. 11 we see that

$$k_1(\alpha, \varepsilon)|_{\alpha=0,\varepsilon=0} = 0, \qquad k_1(\alpha, \varepsilon)|_{\alpha=\pi/18,\varepsilon=0.214} = 0. \tag{39}$$

Therefore, in the vicinity of $\alpha = 0$ and $\varepsilon = 0$, the following zero lift condition is obtainable

$$\frac{\Delta\alpha}{\Delta\varepsilon} = \frac{\pi}{0.214 \cdot 18} 0.816. \tag{40}$$

4 Conclusions

The following conclusions can be drawn:

(1) Regularization of the singular integral equation is an important aspect in applied mathematics as well as in mechanics. This tendency can be found from in more recently published papers [8]—[10]. The investigation presented in this paper is another example of regularising the singular integral equation arising in the thin airfoil problem.

(2) Numerical integration of a non-singular integral can be done without any difficulty, therefore it is convenient to deal with the solution of a weaker singular integral equation. It is proved that very accurate results were obtained in the thin airfoil problem by the use of the proposed approach.

Acknowledgement

The research project is supported by the Science Fund of the Chinese Academy of Sciences.

References

[1] Glauert, H.: Elements of airfoil and aircrew theory. Cambridge: Cambridge University Press 1937.
[2] Kuethe, A. M., Chow, C. Y.: Foundations of aerodynamics. New York: John Wiley & Sons 1976.
[3] Milne-Thomson, L. M.: Theoretical hydrodynamics. London: Macmillan Press 1979.
[4] Chow, C. Y.: Introduction of computational fluid mechanics. (Chinese Translation, Original in English). Shanghai: Shanghai Jiao Tong University Press 1987.
[5] Carey, G. F., Oden, J. T.: Finite elements. Fluid Mechanics **6**, New Jersey: Prentice-Hall 1986.
[6] Prosnak, W. J.: Computation of fluid motions in multiply connected domains. Karlsruhe 1987.
[7] Loitsyanskii, L. G.: Mechanics of liquids and gases. (Chinese Translation, Original in Russian). Beijing: High Education Press 1958.
[8] Cheung, Y. K., Chen, Y. Z.: New integral equation for plane elasticity crack problems. Theor. Appl. Fract. Mech. **7**, 177—184 (1987).
[9] Chen, Y. Z., Cheung, Y. K.: Integral equation approach for crack problem in elastic half-plane. Inter J. Fract. (to appear) (1990).
[10] Ghosh, N., Rajiyah, S., Ghosn, S., Mukherjee, S.: A new boundary element method formulation for linear elasticity. J. Appl. Mech. **53**, 69—78 (1986).

Authors' addresses: Ass. Prof. S. W. Zhang, Division of Applied Mathematics, Jiangsu Institute of Technology, Zhenjiang, Jiangsu, 212013 People's Republic of China, and Prof. Y. Z. Chen, Division of Engineering Mechanics, P.O. Box 80, Jiangsu Institute of Technology, Zhenjiang, Jiangsu, 212013, People's Republic of China.